



Research article

Highly efficient CdS/CeO₂/Ag₃PO₄ nanocomposite as novel heterogenous catalyst for Knoevenagel condensation and acetylation reactions

Fikremariam Chigru Zenebe, Abi M. Tadesse, Muthusaravanan Sivasubramanian, Neelaiah Babu G.*

Department of Chemistry, Haramaya University, Haramaya, Ethiopia

ARTICLE INFO

Keywords:

Heterogeneous catalyst
Knoevenagel condensation
Acetylation
Nanocomposite

ABSTRACT

In light of environmental and economic concerns, the use of heterogeneous catalysts that can function under gentler reaction conditions has recently become popular. In this study by using the precipitation method, CdS/CeO₂/Ag₃PO₄ ternary nanocomposites with varied molar proportions of CdS:CeO₂/Ag₃PO₄ were produced. The catalysts' surface functional groups; morphology and crystal structures were examined using FTIR, SEM-EDX and XRD respectively. The catalytic efficiency of all synthesized nanomaterials was tested on a model Knoevenagel condensation reaction. For the best catalyst, selected from the screening, the optimization of reaction conditions such as the solvent, catalyst load, concentration of reagents such as malononitrile/acetic anhydride, and temperature. The ternary nanocomposite CdS/CeO₂/Ag₃PO₄ (4:1) displayed higher catalytic activity (95.4 ± 3.2 %) than the rest of the nanomaterials prepared. Thus, the ternary nanocomposite CdS/CeO₂/Ag₃PO₄ with 4:1 mol ratio with optimized reaction conditions was used to check the substrate scope of Knoevenagel condensation and acetylation reaction. The synthesized Knoevenagel condensation and acetylation reaction products were also characterized by proton and carbon NMR for their structure determination. The nanocomposite's reusability was carried out and only 7.5 ± 2 % decrement was witnessed after four runs and 23.3 % after the fifth run. and this indicates the potential application of the catalyst to organic reactions. Furthermore, we have proposed the possible catalytic mechanisms for both organic reactions.

1. Introduction

The Knoevenagel condensation is the most prominent reaction for the synthesis of carbon-carbon double bond and it is widely utilized to make a variety of fine chemicals, intermediates, natural and synthetic medicines, cosmetics, and polymers [1,2]. Conventionally, this reaction is performed by using different classes of catalysts such as acids, organic free bases and salts of free bases. Base homogenous catalysts like amines, ammonium salts [3] piperidine, urea [4] etc. and Lewis acid catalysts such as BiCl₃, and CdI₂ [5] serve as the important and widely applied catalytic systems for the Knoevenagel condensation reactions.

The acylation of amines, alcohols, and phenols remains a focal point of research interest because of its fundamental significance and its application in multistep chemical production processes. The acylation reaction is carried out using acylating agents like acetic

* Corresponding author. Department of Chemistry College of Natural and Computational Sciences, Haramaya University, Ethiopia.
E-mail addresses: gnbabu24@gmail.com, neelaiah.babu@haramaya.edu.et (N.B. G.).

<https://doi.org/10.1016/j.heliyon.2024.e31798>

Received 4 March 2024; Received in revised form 21 May 2024; Accepted 22 May 2024

Available online 24 May 2024

2405-8440/© 2024 The Authors. Published by Elsevier Ltd. This is an open access article under the CC BY-NC license (<http://creativecommons.org/licenses/by-nc/4.0/>).

anhydride or acetyl chloride in the presence of basic or acidic catalysts. Base catalysts like, triethylamine, pyridine [6], 4-Dialkylaminopyridines [7], ionic liquid [8], and Lewis acid catalysts such as, $\text{HClO}_4\text{-SiO}_2$ [9], $\text{Ce}(\text{OTf})_3$ [10], $\text{Gd}(\text{OTf})_3$, $\text{Cu}(\text{OTf})_2$, TaCl_5 [11], 4-(*N,N*-Dimethylamino)pyridine. HCl salt [12] have been reported for this reaction.

However, the all the above reported homogeneous catalysts have limitations [13] particularly in terms of challenges with post-reaction problems with separation and adverse environmental impacts. Furthermore, the catalysts fall short of green synthesis standards as they are not recoverable or reusable. Accordingly, given the very high importance of the specialty chemical synthesis, the development of readily separable and reusable catalysts with high catalytic activity is in great demand for cost-effective production of such important chemicals. As a result, the development of heterogeneous catalysts that can be readily separated and reused several times has grown [14].

Recently, nanocatalysis has become a rapidly expanding topic and an essential part of sustainable technology and organic transformations that can be used in all kinds of catalytic organic transformations. The application of nanocatalysts have attracted remarkable attention as reusable, inexpensive, noncorrosive, gives better purities of the products and more environmentally friendly catalysts for various organic transformations under mild and convenient conditions [15]. The catalysts have unique properties due to their nanoscale size, shape, and extraordinarily high surface area to volume ratio.

In heterogeneous catalytic applications, a variety of nano catalysts have been employed, such as nano mixed metal oxides, nano-supported catalysts, and magnetic nano catalysts [16–18]. Metal oxide catalysts often display both electron transport and surface polarizing characteristics, which are directly relevant in redox and acid-base catalytic reactions. Metal oxides like, CeO_2 [19], ZnO_2 [20], $\text{CeO}_2/\text{ZrO}_2$ [21] have been reported for various organic transformations. However, these single and binary nanocatalysts have low thermal stability and moderate catalytic activity. Therefore, the thermal stability and catalytic efficiency of these catalysts are improved by coupling of two or more semiconductors. In this work, we expected that ternary nanocomposites would result in improved catalytic activity as above-mentioned nanocatalytic systems.

Ternary nanocomposites modify the required active sites, surface area and electrical conductivity by synergistically combine the characteristics of three materials. According to Yin and co-workers [22], the ternary nanocomposite exhibited superior durability and reproducibility than binary composites. Zamiri et al., reported that the incorporation of 3DG into the $\text{SnO}_2\text{-TiO}_2$ binary nanocomposite increased its surface area and decrease size compared to the single and binary composite [23]. This results a high adsorption of substrates on the catalyst surface and increase the catalytic processes. Appaturi and co-workers also concluded that nanocomposites with high surface area can increase the Knoevenagel reaction performance [24]. Due to the synergetic effect, Cu-MOF/GO ternary composites showed a higher catalytic activity, better cycling stability and excellent chemical and thermal robustness than pure Cu-MOF or GO . Recently some ternary nanocatalysts such as $\text{CeO}_2/\text{Al}_2\text{O}_3/\text{Fe}_3\text{O}_4$ [25], $\text{ZrO}_2\text{-Al}_2\text{O}_3\text{-Fe}_3\text{O}_4$ [26] for esterification reaction, $\text{Fe}_3\text{O}_4@ \text{UiO-66-NH}_2$ [27] for Knoevenagel reaction and $\text{Ag}/\text{Al}_2\text{O}_3@ \text{Fe}_2\text{O}_3$ [28] for acetylation reaction have been reported. However, up to now, no related report is available on the catalytic activity of $\text{CdS}/\text{CeO}_2/\text{Ag}_3\text{PO}_4$ for any organic reactions. Recently, hybrid materials based on MOFs such as InPb -cluster-based honeycomb framework of $\{[(\text{CH}_3)_2\text{NH}_2][\text{In}^{\text{III}}\text{Pb}^{\text{II}}(\text{TDP})(\text{H}_2\text{O})]\cdot 3\text{DMF}\cdot 3\text{H}_2\text{O}\}_n$ and cobalt-organic framework of $\{[\text{Co}_3(\text{TNBTB})_2(\text{PTP})]\cdot 7\text{DMF}\cdot 6\text{H}_2\text{O}\}_n$ also reported for the heterogeneous catalysis of Knoevenagel condensation reactions of benzaldehyde and malononitrile [29,30].

The primary objective of this research work is to assess the catalytic activity of $\text{CdS}/\text{CeO}_2/\text{Ag}_3\text{PO}_4$ heterogeneous nano catalysts by subjecting to the Knoevenagel condensation reaction and acetylation reactions.

2. Experimental procedures

2.1. Materials

All reagents and chemicals were of reagent grade or better and were used as obtained without further purification.

2.2. Preparation of nanocatalysts

2.2.1. Preparation of CeO_2 nanoparticles

Cerium oxide nanoparticles have been synthesized through the co-precipitation process employing a modified method [31]. 0.1 M equivalent weight of cerium (III) nitrate hexahydrate was dissolved in doubly deionized water and the solution was stirred for 30 min. To the 0.1 M cerium (III) nitrate solution, 25 % ammonia was gradually added dropwise while stirring continuously. The stirring was continued for another 2 h and the pH of the solution has been maintained 10. The reaction was continued for another 12 h to achieve the complete precipitation process. The reaction mixture was further aged for 12 h. The resultant yellow precipitate was centrifuged at 2000 rpm for 30 min, followed by filtration. Subsequently, the precipitate was washed with deionized water and ethanol. The wet yellow CeO_2 precipitate was dried in the oven for 12 h at 140 °C before it was calcined for 3 h at 500 °C.

2.3. Preparation of Ag_3PO_4 nanoparticles

The precipitation method was used to produce silver phosphate nanoparticles, as was previously reported in the literature with minor modifications [32]. AgNO_3 and Na_2HPO_4 were each dissolved in 60 mL of doubly distilled water to prepare separate 0.1 M solutions. The 0.1 M solution of Na_2HPO_4 was gradually introduced into 0.1 M solution of AgNO_3 . The mixture was stirred continuously for 4 h in a dark environment at room temp. Finally, the yellow precipitate obtained was subjected to filter, washed, and then dried in an oven at 60 °C for 6 h. The resulted solid was then calcined for 2 h in a furnace at 300 °C.

2.4. Preparation of CdS nanoparticles

0.1 M $\text{Cd}(\text{CH}_3\text{COO})_2 \cdot 2\text{H}_2\text{O}$ and $\text{Na}_2\text{S} \cdot 9\text{H}_2\text{O}$ solutions were prepared in distilled water in different beakers. The sodium sulfide solution was gradually added to the $\text{Cd}(\text{CH}_3\text{COO})_2 \cdot 2\text{H}_2\text{O}$ solution with constant stirring over a period of 2 h under nitrogen gas purging. Consequently, the resultant yellow precipitate was collected through centrifugation, washed thrice with deionized water and ethanol, and subsequently dried in an oven at 70 °C for a duration of 5 h [33]. The solid product was subjected to calcination for 2 h at 300 °C.

2.4.1. Preparation of $\text{CeO}_2/\text{Ag}_3\text{PO}_4$ nanocomposite

The $\text{CeO}_2/\text{Ag}_3\text{PO}_4$ heterostructured nanocomposite was prepared using an *in situ* precipitation approach with a minor modification from literature report [34]. CeO_2 nanoparticles, at a concentration of 0.0814 mmol, were dispersed in 100 mL of deionized water and subjected to sonication for a duration of 30 min. To the above sonicated solution, 0.1 M of AgNO_3 solution was charged to the white CeO_2 dispersed sonicated solution and continuously stirred for 0.5 h. Then, 0.1 M Na_2HPO_4 solution was gradually added dropwise, accompanied with thorough stirring for 2 h. The reaction contents were subjected to filtration to separate the resulted yellow product and washed three times using deionized water. Thus, obtained yellow product dried for 10 h in an oven at 80 °C.

2.4.2. Preparation of CDS/ CeO_2 nANOCOMPOSITE

0.1 M of the prepared CeO_2 nanoparticles were dispersed in 100 mL of distilled water and sonicated for 30 min. Then 0.1 M $\text{Cd}(\text{CH}_3\text{COO})_2 \cdot 2\text{H}_2\text{O}$ solution was added to the white CeO_2 dispersed solution. After completing 1 h of continuous stirring, 0.1 M $\text{Na}_2\text{S} \cdot 9\text{H}_2\text{O}$ solution was charged dropwise into the above prepared solution. Thus obtained solid product was subjected to filtration and water and ethanol washes were given three times, and then dried in oven at 60 °C for 24 h [35].

2.4.3. Preparation of $\text{CdS}/\text{CeO}_2/\text{Ag}_3\text{PO}_4$ nanocomposite

The ternary nanocomposite $\text{CdS}/\text{CeO}_2/\text{Ag}_3\text{PO}_4$ was prepared by incorporating appropriate quantities of $\text{CeO}_2/\text{Ag}_3\text{PO}_4$ nanocomposite with varying mole ratios of CdS (CdS to $\text{CeO}_2/\text{Ag}_3\text{PO}_4$; 1:1, 2:1, 3:1, and 4:1) in deionized H_2O .

0.1 M $\text{CeO}_2/\text{Ag}_3\text{PO}_4$ nanocomposite was dispersed in deionized H_2O and subjected to sonication for 2 h. To the sonicated solution, 0.1 M $\text{Cd}(\text{CH}_3\text{COO})_2 \cdot 2\text{H}_2\text{O}$ solution was supplemented and the solution was then further subjected to sonication for 1.5 h. To the above solution, 0.1 M $\text{Na}_2\text{S} \cdot 9\text{H}_2\text{O}$ was mixed and the reaction mixture was stirred for another 3 h. The change in colour of the reaction was observed from yellow to blue black precipitate. The whole reaction mixture was centrifuged at 2000 rpm for 0.5 h and the solid was washed with deionized water and ethanol. The solid was then put for drying in an oven at 100 °C for 12 h. Finally, the dried solid was grounded to get fine powder.

2.5. Characterization of the prepared catalysts

The produced nanocatalysts were investigated by XRD by using a Philips X'PERT Pro PANalytical diffractometer with an X'Celerator detector. $\text{Cu K}\alpha$ radiation ($\lambda = 1.5418 \text{ \AA}$) was used to identify the crystalline structure or phase purity. Crystal size was determined using the Scherrer equation. The diffraction patterns were obtained at 2θ values from 4 to 90.

Scanning electron microscopy (SEM) was employed to investigate the morphology and particle distribution of prepared nanocatalysts utilizing a Hitachi TM1000 with EDX and backscattered detectors. The elemental percent weight distribution of the as-synthesized sample has been determined employing energy dispersive X-ray (EDX) with SEM (acquisition time 40.0 s, process duration 3 h, and accelerating voltage 15.0 kV). HRTEM micrographs were obtained by utilizing a JEOL 2100F electron microscope at 200 kV with an INCA x-sight detector from Oxford Instruments. The FT-IR was used to get the information about the existing functional groups of the developed nanocatalysts using an FTIR instrument namely Spectrum 65 by PerkinElmer. The FT-IR transmission spectra was recorded between 4000 and 400 cm^{-1} .

2.6. Optimization of reaction condition

The optimization study was performed on Knoevenagel Condensation reaction. The reaction of benzaldehyde with malononitrile was chosen as a template Knoevenagel condensation reaction. The reaction parameters optimized were temperature, solvents and catalyst load of prepared nanomaterials. The optimization study was also performed for Acetylation reaction. The reaction of aniline and acetic anhydride was opted as template reaction for acetylation. The parameter optimized for acetylation reaction is concentration of acetic anhydride.

2.7. General procedure for the Knoevenagel condensation reaction

To obtain Knoevenagel condensation product, an aromatic aldehyde (1 mmol), malononitrile (1.5 mmol) and the nanocatalyst (5 % w/w catalysts with increasing intervals of 5 % for optimization of catalyst load) were charged in a 100 mL three-neck flask. The reaction contents were continuously stirred in ethanol (2.5 mL) at 25 °C. TLC was used to check the progress of the reaction using hexane:ethyl acetate mobile phase (3.5:1.5). Upon completion of the reaction, the mixture was quenched by pouring ice water to obtain solid Knoevenagel condensed product as precipitate. The remaining ethanol water mixture was subjected suction filtration to separate from the reaction product and catalyst. The Knoevenagel condensed product with nanocatalyst dissolved in methanol and the

nanocatalyst was separated from the Knoevenagel condensed product by simple filtration. The organic phase was dried over anhydrous sodium sulfate. Finally, methanol was evaporation achieved under vacuum to give the Knoevenagel condensed product.

2.8. General procedure for acetylation reaction

For the acetylation of reactants like alcohol, phenol, or amine with as prepared heterogenous catalysts, in a distinctive experimental procedure, 1 mmol of reagent (alcohol/phenol/amine) was charged to a mixture of heterogenous nanocatalyst (15 % w/w) and 2 mmol of acetic anhydride in 2.5 mL acetonitrile solvent. The reaction mixture was continuously stirred at 65 °C for phenol and alcohols and at 25 °C for amines until the reaction completed. The thin layer chromatography was used to check the progress of reaction using hexane:ethyl acetate; 3:2 as mobile phase. Upon the completion of reaction, 10 mL of EtOAc was added and filtered to recover the nanocatalyst. The combined organic phase was subjected to washing with 10 % solution of NaHCO₃ and water two times and dried using sodium sulfate anhydrous. The organic solvent was evaporated to obtain the desired acylated product.

3. Results and discussion

3.1. Characterization of nanocatalysts

3.1.1. XRD analysis of nanocatalysts

The XRD patterns of all the as-synthesized nanocatalysts are shown in Figs. 1 and 2 below. Accordingly, diffraction peaks observed Fig. 1c at 2θ of 28.5, 33.06, 47.45, 56.29, 59.19, 69.29, 76.73, 79.05 and 88.33° corresponding to (111), (200), (202), (311), (222), (400), (313), (402) and (422) lattice plane respectively represents the cubic fluorite structure of CeO₂ [96-434-3162] [26,28]. The diffraction peaks observed from Fig. 1a, at 2θ of 20.88, 29.69, 33.29, 36.58, 42.49, 47.79, 52.68, 55.01, 57.27, 61.64, 65.84, 69.89, 71.88, 73.84, 87.21 and 89.10° can be attributed to (101), (020), (201), (121), (202), (301), (222), (302), (312), (040), (303), (402), (412), (323), (423) and (512) crystal plane indexed to the body centered cubic structure of Ag₃PO₄ [96-153-0490] [36]. The broad peaks observed from Fig. 1e at 2θ of 24.95, 26.53, 28.21, 43.81, 48.02, 52.03, 66.83, 69.51, 70.99, 72.37, 80.53 and 86.53° corresponding to (100), (002), (101), (110), (103), (112), (203), (210), (211), (114), (300) and (213) crystal plane can be ascribed to the hexagonal greenockite structure of CdS nanoparticle [96-101-1055] [37].

The diffraction peaks observed in CdS/CeO₂ (Fig. 1d) binary system at 2θ values of 28.56, 33.09, 47.60, 56.28, 59.18, 69.48, 76.67, 79.13 and 88.46° represents the cubic fluorite structure of CeO₂. And also diffraction peaks at 2θ values of 26.44, 44.58 and 54.84° indicate the presence of hexagonal greenockite structure of CdS in the binary system [35]. Therefore, the characteristic diffraction peaks for both CeO₂ and CdS are observed from the XRD pattern of the BINARY composite, indicating the formation of CdS/CeO₂ composite. For CeO₂/Ag₃PO₄ composite (Fig. 1b), almost all of the diffraction peaks observed could be ascribed to the body centered cubic structure of Ag₃PO₄. The diffraction peak of CeO₂ appear in a weak intensity in the XRD pattern of the CeO₂/Ag₃PO₄ composite which might be due to the small concentration of CeO₂ [34]. The sharp diffraction peaks of the composite indicate their good crystallinity. No traces of other phases are detected, confirming the high purity of the samples.

For the ternary system, different molar ratios of CdS: CeO₂/Ag₃PO₄ composites were characterized and demonstrated in Fig. 2 (a–d). For all ternary systems of CdS: CeO₂/Ag₃PO₄, similar diffraction peaks were observed at 2θ value of 24.89, 26.54, 28.26, 28.79, 29.16, 29.6, 31.72, 33.34, 34.61, 37.0, 38.26, 40.96, 43.62, 46.41, 47.99, 52.63, 53.46, 55.63, 55.14 and 56.87° respectively. Among these, diffraction peaks at 2θ values of 28.79, 29.16, 33.34, 47.99 and 56.87° could be attributed to the cubic fluorite structure of the crystal CeO₂; diffraction peaks at 2θ value of 29.6, 31.72, 33.19, 33.34, 34.61, 37.0, 52.63 and 55.14° could be attributed to body

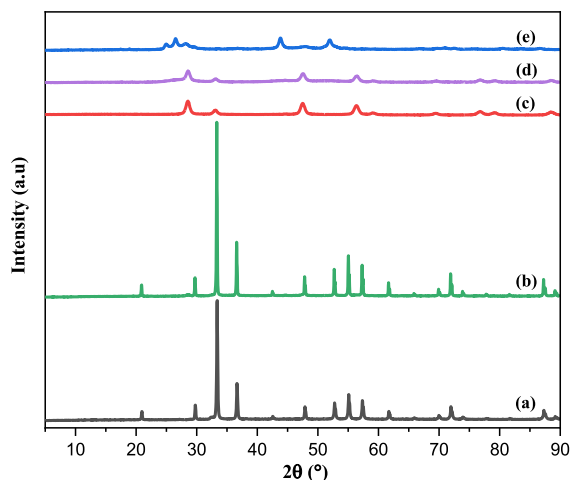


Fig. 1. XRD patterns of (a) Ag₃PO₄, (b) CeO₂/Ag₃PO₄, (c) CeO₂ (d) CdS/CeO₂ (e) CdS nano catalysts.

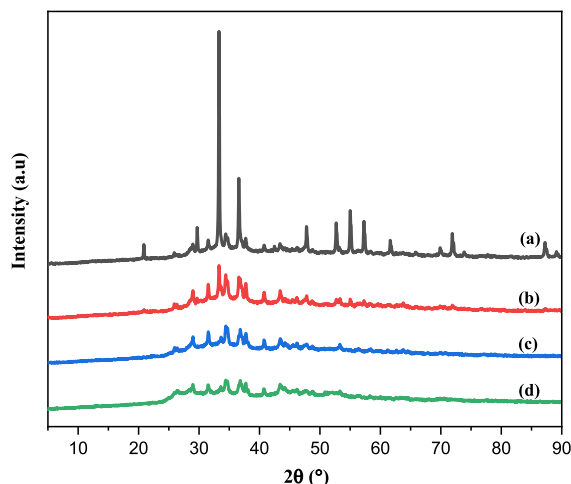


Fig. 2. XRD patterns of (a) CdS/CeO₂/Ag₃PO₄ (1:1), (b) CdS/CeO₂/Ag₃PO₄ (2:1), (c) CdS/CeO₂/Ag₃PO₄ (3:1) (d) CdS/CeO₂/Ag₃PO₄(4:1).

centered cubic structure of Ag₃PO₄ and peaks at 2θ value of 24.88, 26.54, 28.26, 43.62 and 53.46° can be accounted for the hexagonal greenockite structure of CdS nanoparticle.

The average crystallite size of each of the as-synthesized nanocatalysts was calculated using the Debye-Scherrer formula as shown in Equation (1):

$$D = \frac{K\lambda}{\beta \cos \theta} \quad 1$$

Where, D = Crystallite size in nm, K = the shape factor constant taken as 0.9, λ is the wave length of the X-ray (0.15406 nm) for Cu target Kα1 radiation, β is the full width at half maximum (FWHM) in radians and θ is the Bragg's angle in radians.

The calculated average crystalline size of as-synthesized nanocatalysts are summarized in Table 1 below and confirm the involvement the good crystalline range.

3.1.2. SEM-EDX image study

The morphology of the prepared nanocomposite catalyts were investigated by scanning electron microscopy (SEM) as shown in Fig. 3. From Fig. 3a, the morphologies of CdS/CeO₂ composite shown no different morphology, even if cubic like structures looked hardly. And also, the SEM micrograph showed that, CdS/CeO₂ composite is composed of two dissimilar phases. In the case of ternary system (Fig. 3b), the SEM image showed irregular shape with no distinct morphology.

Energy dispersive X-ray spectroscopy (EDX) study of the catalyts is depicted and indicate the existence of all elements. It can be clearly observed that, from the ternary mixtures EDX (Fig. 3c & e) a gradual increment in Cadmium percentage. However, the EDX was not shown the element Ce in CdS/CeO₂/Ag₃PO₄ (3:1) composite (Fig. 3d), though the presence of Ce in the catalyst is clearly indicated in the XRD pattern. This might suggest that the CeO₂ may be masked within the composite (coated on the surface of the composite) since SEM shows the outer surface of crystals. Generally, no other unwanted elements were observed in EDX spectrum of composites, indicating the purity of the phase.

3.1.3. FT-IR analysis of the nanocatalyts

The functional groups of the as-synthesized nanocatalyts, CeO₂, CdS/CeO₂, CdS/CeO₂/Ag₃PO₄ and 4-time reused CdS/CeO₂/

Table 1
Crystallite sizes of the as-synthesized nanocatalyts.

Nanocatalyts	2θ (degree)	β (radians)	D (nm)
CeO ₂	28.5	0.012856	11.1
CdS	43.81	0.012854	11.6
Ag ₃ PO ₄	33.29	0.004674	30.9
CdS/CeO ₂	28.56	0.015193	9.4
CeO ₂ /Ag ₃ PO ₄	33.29	0.005843	24.8
CdS/CeO ₂ /Ag ₃ PO ₄ (1:1)	34.31	0.004674	31.1
CdS/CeO ₂ /Ag ₃ PO ₄ (2:1)	43.38	0.005843	24.9
CdS/CeO ₂ /Ag ₃ PO ₄ (3:1)	34.42	0.007013	20.7
CdS/CeO ₂ /Ag ₃ PO ₄ (4:1)	34.34	0.007013	20.7

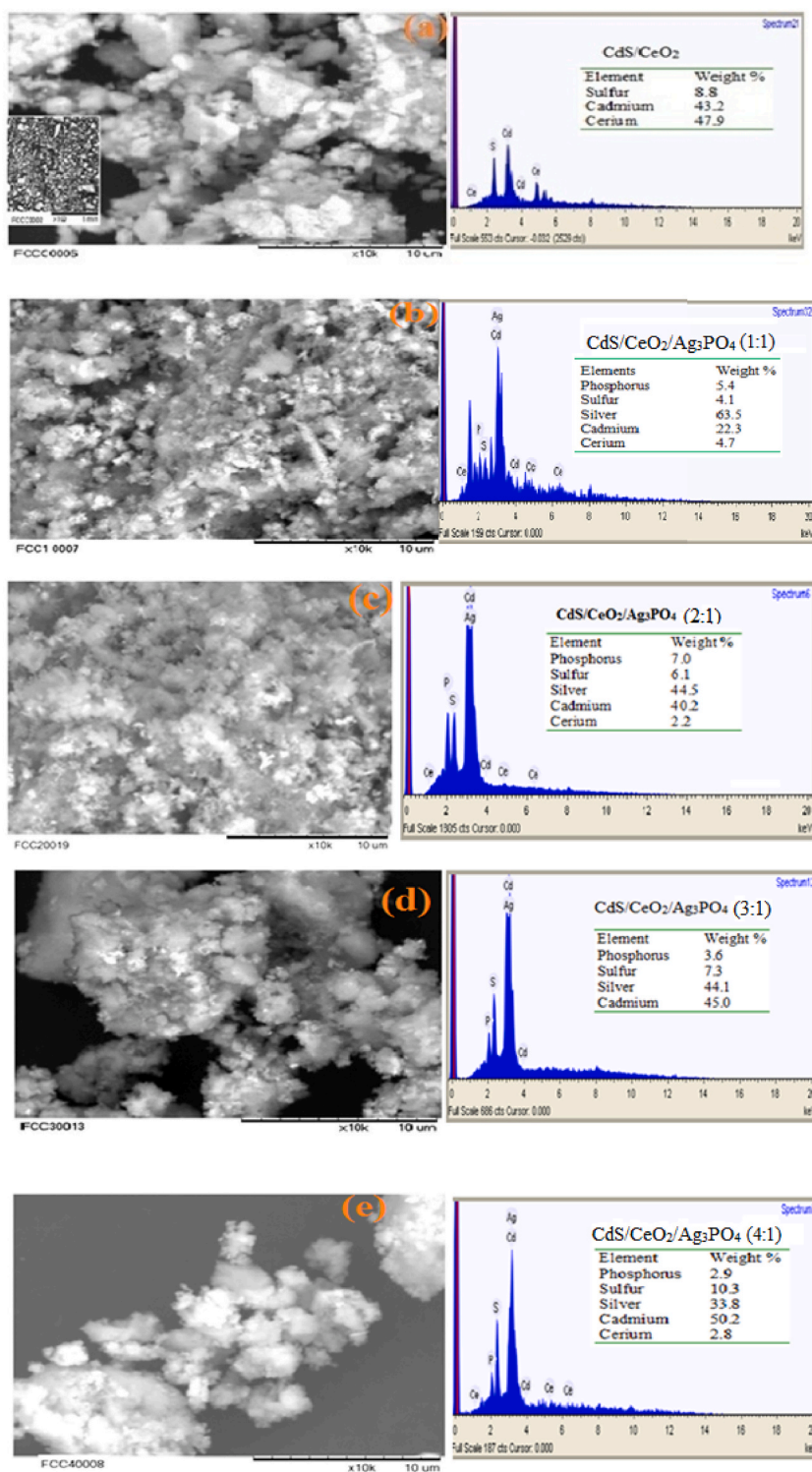


Fig. 3. SEM images and corresponding EDX of (a) CdS/CeO₂, (b) CdS/CeO₂/Ag₃PO₄ (1:1), (c) CdS/CeO₂/Ag₃PO₄ (2:1), (d) CdS/CeO₂/Ag₃PO₄ (3:1) and (e) CdS/CeO₂/Ag₃PO₄ (4:1).

Ag₃PO₄ catalyst were examined by FT-IR spectrometer in the range of 4000 to 400 cm⁻¹ and exhibited in Fig. 4. All samples showed broad band around 3433 cm⁻¹ could be ascribed to the O–H stretching vibration of the physical adsorbed water molecules on the nanocatalyst surface. The band situated around 1624 cm⁻¹ is corresponded to the bending mode of the hydroxyl group (adsorbed

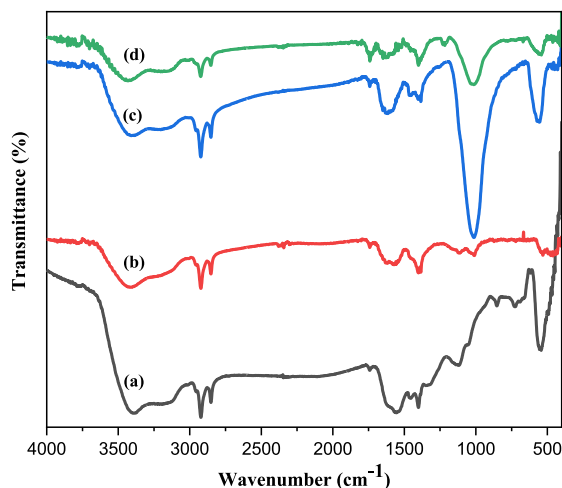


Fig. 4. FTIR spectrum of (a) CeO₂ (b) CdS/CeO₂ (c) CdS/CeO₂/Ag₃PO₄(4:1) (d) CdS/CeO₂/Ag₃PO₄(4:1) after four recycle.

water) [38]. Weak Peaks observed at 2851 and 2922 cm⁻¹ can be attributed to symmetric and asymmetric C–H str. vibrations, which might be credited to the impurities of KBr [39]. Weak Peaks observed at 1385 cm⁻¹ attributed to the N=O stretching vibration that was produced by the trace amount of nitrate which resulted from the residual solution of Ce(NO₃)₃·6H₂O [40]. Strong absorption peak observed at 1014 cm⁻¹ corresponds to P–O stretching vibrations of the phosphate groups (PO₄³⁻) resulted from Ag₃PO₄ [34,41]. As presented in Fig. 4a, the FT-IR spectrum of CeO₂ shows a band at 552 cm⁻¹ attributed to the Ce–O vibration of the CeO₂ crystal. It is evident from the FTIR data that the Ce–O vibrational mode was more prominently observed [40]. The CdS/CeO₂ FT-IR spectrum (Fig. 4b) indicated that the formation of the desired binary nanocomposite. The FT-IR result (Fig. 4d) for the 4-time reused CdS/CeO₂/Ag₃PO₄ catalyst showing no structure alternation which showed the great stability of the catalyst. On comparison with fresh CdS/CeO₂/Ag₃PO₄ (Fig. 4c) and four times used ternary nanocomposite (Fig. 4d), in both the fingerprint region and functional group region hardly any difference in pattern can be observed. This no change in pattern indicates the ability of reusability of this nanocatalyst.

3.2. Catalytic applications

3.2.1. Catalytic studies of the as-synthesized nanocatalysts for Knoevenagel condensation reaction

Numerous amines, Lewis acids, or acid-base bifunctional catalysts can catalyze the Knoevenagel reaction because of the synchronized activation of carbonyl functionality on acid sites and uptake of the proton from CH₂ group on base reactive sites [39]. The yield was used to compare the catalytic performance of the investigated nanocatalysts and serve as a gauge of catalytic activity.

Optimization of reaction condition; The Knoevenagel condensation reaction of benzene carboxaldehyde and malononitrile at room temperature was used as the model reaction for the optimization of reaction parameters. The effect of the solvent on Knoevenagel condensation reaction catalyzed by 0.1 g of CdS/CeO₂/Ag₃PO₄ (4:1) was examined and the outcomes were given in Table 2. The use of methanol and ethanol produced good yield of 2-benzylidenemalononitrile. While water is a preferred solvent for chemistry reactions due to affordability, safety, and environmental issues, the model Knoevenagel condensation reaction use of water as a solvent yielded poorly with long reaction time (Entry, 4). The significant differences in activity are likely due to the solvents' polarity and their amphiprotic properties.

Bhanja et al. [42] have synthesized *p*-chlorobenzylidene-malononitrile in high yields (98 %) using ethanol as solvent at room temperature. Therefore, based on its availability, less toxicity and less cost, ethanol was chosen as a solvent to validate and optimize the remaining parameters like the amount of catalyst, malononitrile quantity for the Knoevenagel condensation reaction.

After the solvent was selected, the concentration of the malononitrile was optimized with 0.1 g of CdS/CeO₂/Ag₃PO₄ catalyst at

Table 2
Influence of solvents on Knoevenagel condensation reaction.

Entry	Solvent	Time (min)	Yield (%)
1	Methanol	31	95.4
2	Toluene	28	87.2
3	Ethanol	32	94.9
4	Water	180	80

^a Isolated yield after purification by column chromatography.

Reaction conditions: Benzaldehyde (1 mmol), malononitrile (1.5 mmol), catalyst (15 mg), rt.

room temperature. The influence of reactants ratio (benzaldehyde to malononitrile) on the Knoevenagel condensation reaction was studied at different molar ratios *viz.* 1: 0.5, 1:1, 1:1.5 and 1:2. The results, which are summarized in Fig. 5, exhibited that in the presence of 1.5 mmol of malononitrile, the best yield of 2-benzylidenemalononitrile (94.4 % in 50 min) was obtained. But further increasing of amount of malononitrile did not improve the yield. Therefore, 1:1.5 M ratio of benzaldehyde: malononitrile was used for further Knoevenagel reactions.

Effect of catalyst load: Initially a control experiment was carried out to determine the rate of the reaction. As can be seen in Table 3 (entries 1), with out the use of the catalyst, 2-benzylidenemalononitrile was produced in poor yield (48.1 %) despite long reaction time (4.1h). When the amount of CdS/CeO₂/Ag₃PO₄ (4:1) nanocatalyst was increased, a significant improvement of the conversion was observed as expected. The yield shows a significant increase from 75.8 to 95.0 %; however, there is no notable difference between entries 4 and 5 (Table 3). This suggests that the catalyst quantity in entry 4 (Table 3) is optimal for future reactions when considering both catalyst amount and reaction time. In all case the catalysts had good catalytic activity even at lower catalyst loading (5 % w/w). Cerium oxide's redox and acid-base properties, whether alone or in combination with transition metals, play a significant role in activating and selectively transforming organic compounds [43].

After the determination of the optimum catalyst load, temperature effect was investigated (Table 4). Table 4 illustrates the impact of temperature at 25, 40, and 65 °C. As the increase in temperature was adjusted to 65 °C, a fair increment in yield was observed. But the yield of product for an increase of temperature from 25 to 65 °C showed maximum of 3 % difference. Since the yield increment is not significant with higher temperature and specified laid down principles of green chemistry, we opted to carry out further reactions at room temperature.

After the optimization of the reaction conditions by CdS/CeO₂/Ag₃PO₄ (4:1) catalyst, we compared this particular composition with the same ternary system but different composition to ensure the one we selected is better. Besides, we want to be sure if this ternary system is better than its single and binary congeners. Accordingly, single and binary counterparts; and in addition three more ternary systems of the same composite at different proportions, CdS/CeO₂/Ag₃PO₄ ternary nanocomposite (1:1, 2:1, 3:1 and 4:1), were synthesized and employed for the same reaction the result of which is depicted in Table 5. The findings indicate that the catalytic efficiency of both binary and single nanocatalysts enhances in this sequence: CdS/CeO₂ > CeO₂/Ag₃PO₄ > CeO₂ > CdS > Ag₃PO₄. Compared to single and binary nanocatalysts, the ternary nanocomposite CdS/CeO₂/Ag₃PO₄ demonstrated superior catalytic performance. As indicated below in Table 5, The increase in catalytic efficiency from a single nanocatalyst to binary, and from binary to ternary, unequivocally shows that coupling creates a state conducive to the enhancement of conversion efficiency.

Reaction condition: Benzaldehyde (1 mmol), malononitrile (1.5 mmol), catalyst (15 % w/w), solvent (2.5 mL), room temperature (25 °C). Lit M.P. = 82–85 °C [44].

The ternary nanocomposite CdS–CeO₂/Ag₃PO₄ (4:1 M ratio) presented highest catalytic activity compared to rest of the catalytic systems and henceforth nominated for further studies. This might be attributed to the tiny particle size (Table 1), which provides a large surface area for reaction adsorption and so exhibits high catalytic activity [45]. Finally, it is concluded that, the improved catalytic activity of CdS/CeO₂/Ag₃PO₄ (4:1) is due to the highest load of CdS on CeO₂/Ag₃PO₄ nanoparticles. The activity of pure CeO₂ was greater than Ag₃PO₄ and CdS might be due to its slight particle size and higher coordination of the Ce⁴⁺–O²⁻ acid-base pair sites on the surface that participate efficiently in the catalysis of deprotonation and dehydration steps.

For comparison, homogeneous catalyst like urea on the Knoevenagel condensation was investigated (Table 5, Entry 1). Although very good yield is obtained, the reaction time was longer and it was difficult to recover and reuse in industrial procedure for possible multiple usage.

With improved reaction conditions from optimization experiments, the catalytic activity of CdS/CeO₂/Ag₃PO₄ (4:1) nanocatalyst was too investigated for various aldehydes with malononitrile using ethanol as solvent (Table 6). In every instance, the reactions yielded high to exceptional results within significantly reduced time frames. (Table 6). The enhanced cooperative effect of the nanocatalyst's acidic and basic sites, along with the abundance of active sites, might account for this phenomenon in the reaction.

Contrary to aromatic aldehydes that have an electron-donating group, like a OH group, at the *p*-position (entry 1, Table 6), those with electron-withdrawing groups as substituents, such as a nitro group at the 2 and 3-positions (entries 2 and 3, Table 6), have shown excellent yields. The reason for this kind of trend could be due to electron-donating groups enhancing the electron density of the aldehyde moieties, thereby hindering their interaction with activated malononitrile [2]. The reaction times and yield with 2-NO₂

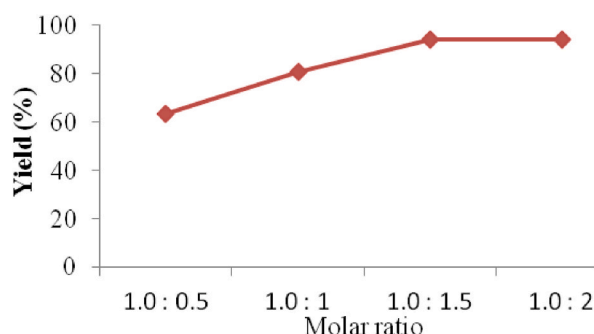


Fig. 5. Effect of molar ratios of benzaldehyde: malononitrile at 50 min.

Table 3
Effect of catalyst loading in the Knoevenagel condensation reaction.

Entry	Catalyst load (g, % w/w)	Average Time (min)	Average Yield	m.p. (°C)
1	Catalyst free	246	48.1	80–81
2	CdS/CeO ₂ /Ag ₃ PO ₄ (0.025, 5)	31	75.8	81–84
3	CdS/CeO ₂ /Ag ₃ PO ₄ (0.0498, 10)	23	89.8	83–85
4	CdS/CeO₂/Ag₃PO₄ (0.0747, 15)	26	95.0	81–84
5	CdS/CeO ₂ /Ag ₃ PO ₄ (0.0996, 20)	27	95.3	81–85
6	CdS/CeO ₂ /Ag ₃ PO ₄ (0.1245, 25)	29	90.6	84

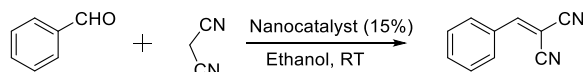
Reaction conditions: Benzaldehyde (1 mmol), malononitrile (1.5 mmol), catalyst (5 % w/w interval), solvent (2.5 mL), room temperature (25 °C). Literature M.P = 82–85 °C [44].

Table 4
Effect of temperature toward Knoevenagel condensation.

Nanocatalyst	Temperature (°C)	Average Time (min)	Average Yield (%)	m.p. (°C)
CdS/CeO ₂ /Ag ₃ PO ₄ (4:1)	25	28	95	81–84
	40	27	95.9	80–84
	65	28	96.4	81–83

Reaction condition: Benzaldehyde (1 mmol), malononitrile (1.5 mmol), Catalyst (15 %), Ethanol (2.5 mL). Lit M.P. = 82–85 °C [44].

Table 5
Effect of different catalysts on the Knoevenagel condensation.



Entry	Catalysts	Time (min)	Yields (%)	m.p. (°C)
1	Urea	71	96	82–83
2	CeO ₂	66 ± 6.6	83.5 ± 3.9	80–83
3	CdS	64 ± 2.6	83.1 ± 4.6	81–84
4	Ag ₃ PO ₄	73 ± 6	78.8 ± 3.3	79–83
5	CdS/CeO ₂	49 ± 4	88 ± 2.1	84–85
6	CeO ₂ /Ag ₃ PO ₄	58 ± 2.6	85.6 ± 2.8	84
7	CdS/CeO ₂ /Ag ₃ PO ₄ (1:1)	51 ± 6	88.2 ± 2.5	81–82
8	CdS/CeO ₂ /Ag ₃ PO ₄ (2:1)	43.7 ± 3.8	89.3 ± 0.9	82–84
9	CdS/CeO ₂ /Ag ₃ PO ₄ (3:1)	33.7 ± 5.0	93.2 ± 1.9	83–84
10	CdS/CeO ₂ /Ag ₃ PO ₄ (4:1)	33.3 ± 3.1	95.4 ± 3.2	83–86

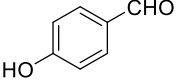
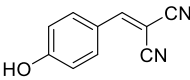
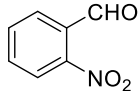
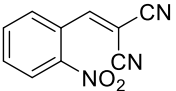
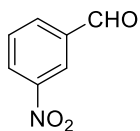
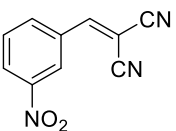
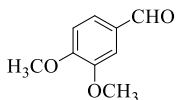
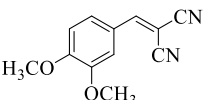
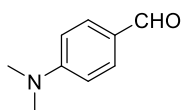
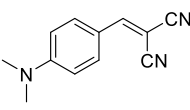
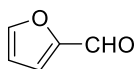
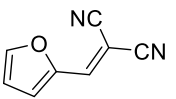
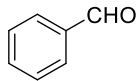
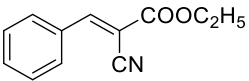
benzaldehyde is lower than that one with 3-NO₂ benzaldehyde suggesting 2-NO₂ benzaldehyde is more steric hindered than 3-NO₂ benzaldehyde. CdS/CeO₂/Ag₃PO₄(4:1) catalyzed Knoevenagel condensation of benzene carboxaldehyde with ethyl cyanoacetate (*pKa* = 9) was also performed to check the efficiency of the optimized reaction condensation. Ethyl cyanoacetate with *pKa* value of 9 gave better yield (*i.e.* 98 %) than the malononitrile (*pKa* = 11). This proves that, the more acidic the active methylene is used the better will be yield. This result is also comparable with a recent report.

3.2.1.1. Comparison of different catalysts for Knoevenagel condensation reaction. From Table 7, Even though several previously published catalysts showed effective catalysis, maximum of the informed catalytic systems require higher temperature, long reaction time and less reusability to attain exceptional catalytic performance. However, the prepared CdS/CeO₂/Ag₃PO₄ catalyst showed a comparable yield, good reusability and better reaction time at room temperature.

3.2.1.2. Proposed mechanism for Knoevenagel condensation. This catalytic reaction, like other heterogeneous catalytic reactions, occurs on the catalyst surface. In practical terms, the surface atoms operate as Lewis acid-base centers, allowing chemical reactions to be catalytically activated. The key mechanism for catalyzing the reactions is the incidence of strong Lewis acid and base sites on the catalyst surface and the catalyst's high specific surface area [42]. The mechanism using the as-synthesized nanocatalyst illustrated in Fig. 6 was proposed based on formerly reported mechanisms [45] and our observations in the development of the present reaction.

With in this proposed mechanism, the base sites on surface of the catalyst abstract a proton from the active methylene carbon of malononitrile, forming a carbon anion. The acidic sites on the surface of catalyst activate the carbonyl of aldehydes, which results in the formation of carbocation. A dehydration process happens by the carbon anion attacking the carbon cation. Then the product was

Table 6Knoevenagel condensation between various aldehydes and malononitrile^a/ethyl cyanoacetate^b catalyzed by CdS/CeO₂/Ag₃PO₄ (4:1).

Entry	Substrates	Products	Time (min)	Yields (%)	m.p. (°C)	
					Observed	Reported
1			43 ± 3	85 ± 0.4	185–186	187-188 [26]
2			61.3 ± 3.1	93.1 ± 1.7	135–137	136-138 [46]
3			56 ± 2.6	96.2 ± 0.8	100–103	102-104 [47]
4			81.7 ± 2.3	90.9 ± 1.2	162–164	161-163 [48]
5			65.3 ± 2.1	88.7 ± 2.3	176–179	179-180 [26]
6			72.7 ± 4.6	82.4 ± 0.9	67–69	70 [49]
7			38.2 ± 4	98 ± 0.4 ^b	48–49	47-48 [50]

^a Reaction conditions: Aldehyde (1 mmol), malononitrile (pKa = 11, 1.5 mmol), CdS/CeO₂/Ag₃PO₄ (4:1) (15 % w/w, solvent (2.5 mL), room temperature.

^b Reaction conditions: Aldehyde (1 mmol), ethyl cyanoacetate (pKa = 9, 1.5 mmol), CdS/CeO₂/Ag₃PO₄ (4:1) (15 % w/w, solvent (2.5 mL), room temperature.

Table 7Efficiency comparison of CdS/CeO₂/Ag₃PO₄ with reported catalysts.

Entry	Catalysts (reusability)	Solvent	Temperature (°C)	Time (h)	Yield (%)	References
1	CdS/CeO ₂ /Ag ₃ PO ₄ (>5 times)	Ethanol (2.5 mL)	25	0.56	95.4 ± 3.2	Present work
2	Polyoxoniobates (4 times)	Ethanol (1 mL)	25	0.75	98	[51]
3	Fe ₃ O ₄ @SiO ₂ -PVAm (10 times)	Ethanol (5 mL)	rt	0.5	95	[52]
4	MgO/HMCM-22 (3 times)	Ethanol (10 mL)	80	2	96.4	[53]
5	Graphene oxide (5 times)	Solvent-free	rt	4	97	[54]

formed by subsequent elimination of water.

3.2.2. Catalytic activity of CdS/CeO₂/Ag₃PO₄ catalyst for acetylation reactions

The catalytic activity the as-prepared CdS/CeO₂/Ag₃PO₄ nanocatalyst was also tested for the acetylation of amines, alcohol and phenol. Firstly, the impact of the concentration of Acetic anhydride on the reagent conversion into product was considered by carrying out the reaction between aniline and Acetic anhydride at molar ratios of 1:0.5, 1:1, 1:1.5, 1:2 and 1:2.5 respectively in 15 % w/w of catalyst amount (Fig. 7). The outcomes showed that in the occurrence of 2 mmol of Ac₂O, (Aniline: acetic anhydride, 1:2) the catalyst provided the finest yield of 92.9 % in 45min. Upon further increasing the amount of acetic anhydride, the yield remains almost the same. Therefore, Aniline: acetic anhydride, 1:2 M ratio (2 mmol of Ac₂O) was used for further acetylation reactions.

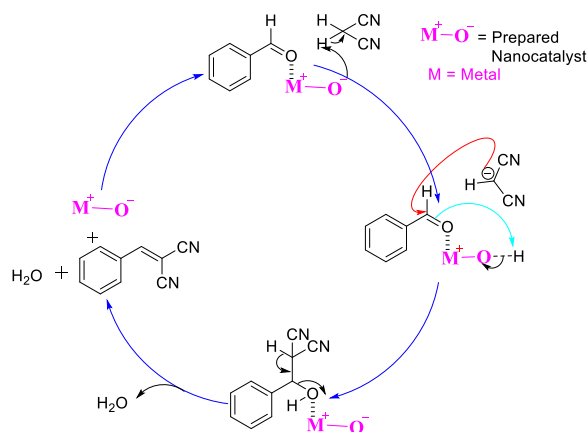


Fig. 6. Plausible mechanism for Knoevenagel reaction catalyzed by CdS/CeO₂/Ag₃PO₄ (1:4).

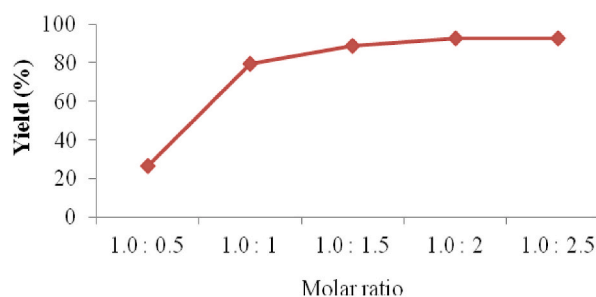


Fig. 7. The effect of molar ratios of aniline: acetic anhydride towards acetylation.

A variety of anilines with different electron donating and withdrawing groups were treated with 2 mmol of acetic anhydride (Table 8). The extremely low yield of acetanilide (44.4 %, Entry 1 below) found in the time off of the catalyst at long reaction times showed the crucial function that the catalyst played in the process. For comparison, homogeneous catalyst like pyridine was investigated (Table 8, Entry 1). However, it was difficult to recover and reuse for other reactions and the product possessed unpleasant odor. While the as synthesized nanocatalyst as shown in Table 8, showed a comparable yield of acetanilide with pyridine and can be separated by simple filtration, reused for further reactions and also the product didn't possess unpleasant odor.

In all cases, good to high yields (83.5 ± 2.1 – 92.9 ± 2 %) of the corresponding acetylated derivatives were obtained. The increased catalytic activity of the ternary nanocomposite can be due to better coordination of the acetic anhydride carbonyl group to the catalyst, since more surface Lewis acidic sites participate in the reaction process [55].

Based on the melting point data (172–175 °C, Lit. 175–177 °C), with 2 mmol of acetic anhydride (Table 8, entry 5), the amino group was selectively acetylated in presence of the –OH group at room temperature. This may be owing to the lower nucleophilicity of the hydroxyl group than the amino group [61]. In these reactions, pleasant smelling esters were the only identified products and, the catalyzed reaction was much faster than the uncatalyzed one. The acetylation of benzyl alcohol and phenols was also investigated. In Blank reactions (in the absence of nanocatalyst), The acetylation of benzyl alcohol under identical reaction conditions produced low yield (15.9 %) at a long reaction time.

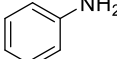
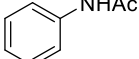
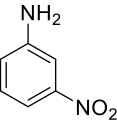
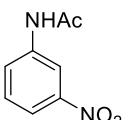
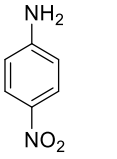
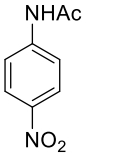
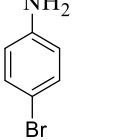
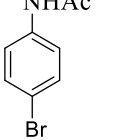
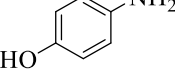
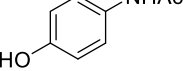
As shown in Table 9, in the presence of CdS/CeO₂/Ag₃PO₄ (4:1) nanocomposite, good average yield of benzyl acetate (86 %) was obtained in less time compared to the blank. This result could be due to more surfaces Lewis acidic sites of the nanocomposite that participating at the reaction. Acetylation of phenol required a longer reaction time than benzyl alcohol. The disproportion in reaction times is ascribed to the lower nucleophilicity of phenols relative to benzyl alcohol, owing to the delocalization of the lone electron pairs on the phenolic oxygen across the benzene ring [62].

The acetylation of 1-naphthol (Table 9, entry 4) was more slowly than other phenol, suggesting a possible steric hindrance.

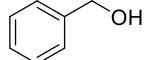
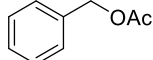
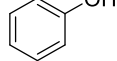
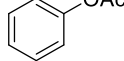
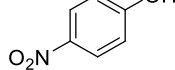
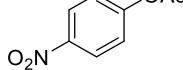
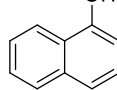
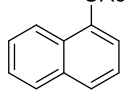
3.2.2.1. Comparison of different catalysts for acetylation reaction. From Table 10, Even though several previously published catalysts showed good catalysis, almost all the recent literature catalytic systems require higher temperature, long reaction time or low product yield and less reusability to obtain excellent catalytic performance. Therefore, as shown in Table 10 below, the reaction condition of the present method was better or comparable with that of most reported method.

3.2.2.2. Mechanism for acetylation reactions. Although the precise mechanism for this reaction over CdS/CeO₂/Ag₃PO₄

Table 8Acetylation of amine with acetic anhydride over the CdS/CeO₂/Ag₃PO₄ (T4) nanocomposite.

Entry	Amine	Product	Time (min)	Yields (%)	m.p. (°C)	
					Observed	Reported
1.			307	44.4 ^a	113–116	112-115 [56]
			2.	94.2 ± 1.3 ^b	112–114	
			61.3 ± 3.1			
			3.	92.9 ± 2 ^c	113–115	
4.			39.4 ± 3.1			152-156
			29.7 ± 2.5	90.9 ± 2.5	152–156	
5.			21.4 ± 1.5	92.3 ± 0.8	212–214	214-216 [58]
6.			50.7 ± 2.6	88.5 ± 2.4	171–173	170-180 [59]
7.			65.3 ± 3.5	83.5 ± 2.1	172–175	175-177 [60]

Reaction conditions: Amine (1 mmol), CdS/CeO₂/Ag₃PO₄ (4:1) catalyst (15 % w/w), Ac₂O (2 mmol), Acetonitrile (2.5 mL), room temperature.^a Yield with catalyst free.^b Yield with pyridine as catalyst.^c Yield with Prepared Catalyst.**Table 9**Acetylation of Phenol and alcohol over the CdS/CeO₂/Ag₃PO₄ (4:1) nanocomposite.

Entry	Substrates	Product	Time (min)	Yields (%)	b.p./m.p. (°C)	
					Observed	Reported
1.			627	15.9 ± 2 ^a	204–206	206 [63]
			2.	86 ± 0.8 ^b		
			35.5			
3.			67	84.7 ± 1.5	194–196	196 [64]
4.			67.5	83.4 ± 1.3	79–81	79 [65]
5.			93	81.8 ± 2.4	41–43	40 [65]

Reaction conditions: Alcohol/Phenol (1 mmol), CdS/CeO₂/Ag₃PO₄ (4:1) catalyst (15 % w/w), Ac₂O (2 mmol), Acetonitrile (2.5 mL), 65 °C.^a Isolated yield with catalyst free.^b Yield with prepared catalyst.

Table 10
Comparison of the proposed catalyst with reported catalysts for the acetylation reaction.

Substrate	Catalysts	Reaction condition	Yield (%)	References	
Benzyl alcohol	Borated zirconia with acetic acid as acetylating agent	Toluene, 110 °C, 14 h	25	[62]	
Phenol			10		
Aniline	ZnAl ₂ O ₄ @SiO ₂	Solvent free, rt, 3 min	96	[55]	
Benzyl alcohol			Solvent free, 75 °C, 20 min		92
Phenol	DMAP·HCl	Toluene (20 mL), rt, 6h	86	[12]	
Benzyl alcohol			Solvent free, 75 °C, 38 min		98
Phenol	α-Zirconium phosphate (ZP)	Toluene (20 mL), rt, 10h	99	[66]	
Benzyl alcohol			Solvent free, 60 °C, 30 min		75
Phenol	CdS/CeO ₂ /Ag ₃ PO ₄	Acetonitrile (2.5 mL), rt, 39.4 ± 3.1min	70	Present work	
Aniline			Acetonitrile (2.5 mL), 65 °C, 35.5min		92.9 ± 2
Benzyl alcohol			Acetonitrile (2.5 mL), 65 °C, 67min		86
Phenol			84.7		

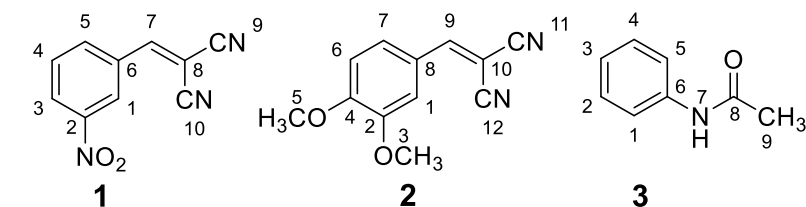
nanocomposite is unclear, we believe it resembles other catalysts as described in the literature [55].

In step one of the mechanism as presented in Fig. 8, the acetic anhydride and substrates are adsorbed on the catalyst surface. The reaction initiates when the acetic anhydride's carbonyl group coordinates with the metal ions on the nanocatalyst's surface, functioning as Lewis acidic sites. The low reactive electrophile is then transformed into a moderately or highly reactive electrophile as a result of the coordination of carbonyl groups to acidic sites on the catalyst surface. Following that, the activated carbonyl group is attacked by a reactive nucleophile, a heteroatom (N or O) of the amine or alcohol, to form the final corresponding acetate and free the catalyst for the next catalytic cycle.

The CdS/CeO₂/Ag₃PO₄ (4:1) catalyst was also applied for Darzens reactions between Bromoacetophenone and aromatic aldehydes and Aldol reaction between acetophenone and aromatic aldehydes at room temperature and 45 °C. However, no product was formed and the reason was not clear and this will be helpful for us as future direction.

3.3. Characterization of the synthesized organic products

The conversion and purity of the organic compounds were checked with TLC and with their melting and boiling point. Beside the TLC and melting point, the structural characterization (identity) and purity of some synthesized organic compounds were determined spectroscopic techniques like ¹H NMR, ¹³C NMR and Dept-135 spectrum in DMSO-*d*₆ as a solvent.



2-(3-Nitrobenzylidene)Malononitrile (1): Off-white crystalline powder, ¹H NMR (400 MHz, DMSO-*d*₆): δ_{ppm} 8.65 (1H, s, H1), 8.46

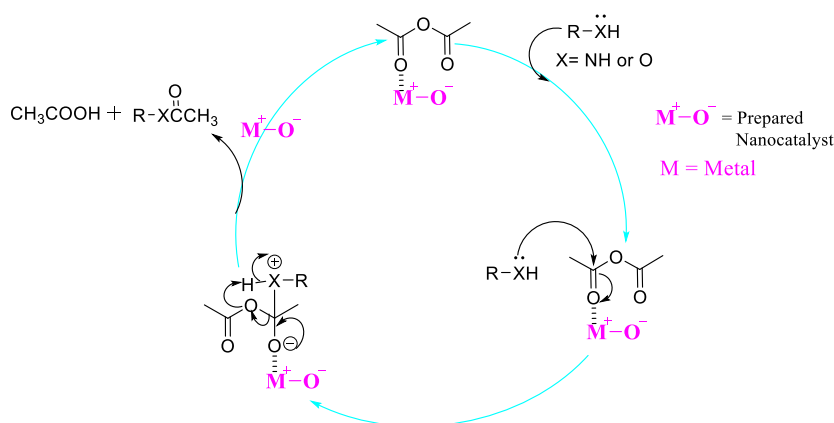


Fig. 8. Plausible mechanism for the acetylation reaction over CdS/CeO₂/Ag₃PO₄ (4:1) catalyst.

(1H, *dd*, H3), 8.31 (1H, *d*, H5), 7.97 (1H, *s*, H7), 7.89 (1H, *t*, H4); ^{13}C NMR (100.6 MHz, DMSO- d_6): δ_{ppm} 159.67, 148.43, 136.32, 132.85, 131.58, 128.34, 125.25, 114.06, 113.01, 85.33; DEPT – 135 (100.6 MHz, DMSO- d_6): δ_{ppm} 154.93, 149.21, 127.81, 115.26, 114.48 and 77.01.

2-(3,4-Dimethoxybenzylidene)Malonitrile (2): Off-white crystalline powder, ^1H NMR (400 MHz, DMSO- d_6): δ_{ppm} 8.29 (1H, *s*, H9), 7.59 (1H, *s*, H1), $\delta_{7.55}$ (1H, *d*, H7), 7.18 (1H, *d*, H6), 3.88 (3H, *s*, H4), 3.78 (3H, *s*, H2); ^{13}C NMR (100.6 MHz, DMSO- d_6): δ_{ppm} 160.98, 154.93, 149.21, 127.81, 124.59, 115.26, 114.48, 112.37, 77.01, 56.48, 55.88; DEPT – 135 (100.6 MHz, DMSO- d_6): δ_{ppm} 154.93, 149.21, 127.81, 115.26, 114.48 and 77.01.

Acetanilide (3): white crystalline powder, ^1H NMR (400 MHz, DMSO- d_6): δ_{ppm} 9.95 (1H, *s*, NH), 7.63 (2H, *d*, H1 and H5), 7.29 (2H, *t*, H2 and H4), 7.02 (1H, *t*, H3), 2.09 (3H, *s*, H9); ^{13}C NMR (100.6 MHz, DMSO- d_6): δ_{ppm} 168.86, 139.77, 129.07, 123.46, 119.54, 24.40; DEPT – 135 (100.6 MHz, DMSO- d_6): δ_{ppm} 168.86 and 139.77.

3.4. Catalytic reusability of the as-synthesized nanocatalyst

The nanocatalyst's reusability study was performed by choosing a Knoevenagel condensation reaction between 3-Nitrobenzaldehyde and malonitrile. The results of recyclability study were presented in Fig. 9. As the reaction completed, identified by TLC, the nanocatalyst was readily collected from the round bottom flask of the reaction with centrifugation and subjected to washings with methanol, subsequently dried at 60 °C for an hour.

Although the reaction time become increased in each cycle, the result indicates the catalyst could be easily recovered and reused four times without a significant loss of activity (only 0.6–6.9 ± 1.3 % loss over the cycles or 7.5 ± 2 % decrement from the initial) in the Knoevenagel condensation reaction. This showed that the catalyst is easily recoverable, stable and appropriate for recycle. The FT-IR spectrum of the catalyst which is not used to the reaction and recycled catalyst (four times) are similar, showing that no substantial changes in chemical or physical properties have been takes place in the prepared nanocatalyst.

4. Conclusion

In summary, we have developed reusable, stable and environmentally friendly catalysts with average sizes in the range 5.9–31.4 nm for the Knoevenagel condensation and acetylation reactions. The nanocatalysts were synthesized by simple co-precipitation method, which is easy, simple, and inexpensive, and less time consuming. Furthermore, the catalysts virtually leave no residue in the reaction media, and the purification methods are simpler than the traditional techniques, which lowers the cost of a potential industrial scale manufacturing. Under the optimal reaction condition, a variety of aldehyde, amine and phenol compounds were converted to the corresponding product in good yields. A proper mechanism for each reaction was also proposed to speculate the chemical reaction process.

Data availability

Data will be made available on request.

CRediT authorship contribution statement

Fikremariam Chigru Zenebe: Writing – original draft, Project administration, Methodology, Investigation, Data curation. **Abi M. Tadesse:** Writing – review & editing, Supervision, Project administration, Funding acquisition, Conceptualization. **Muthusaravanan Sivasubramanian:** Writing – original draft, Methodology, Investigation, Formal analysis, Data curation. **Neelaiah Babu G:** Writing – review & editing, Supervision, Data curation, Conceptualization.

Declaration of competing interest

The authors declare that they have no known competing financial interests or personal relationships that could have appeared to

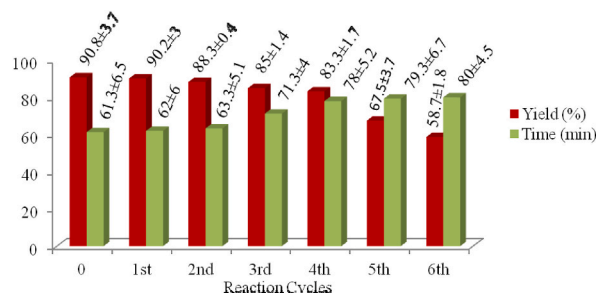


Fig. 9. Results of recycling tests of CdS/CeO₂/Ag₃PO₄ (4:1) nanocatalyst.

influence the work reported in this paper.

Appendix A. Supplementary data

Supplementary data to this article can be found online at <https://doi.org/10.1016/j.heliyon.2024.e31798>.

References

- [1] E.M. Schneider, M. Zeltner, N. Kränzlin, R.N. Grass, W.J. Stark, Base-free Knoevenagel condensation catalyzed by copper metal surfaces, *Chem. Commun.* 51 (2015) 10695–10698.
- [2] C.I. Ezugwu, B. Mousavi, M.A. Asraf, Z. Luo, F. Verpoort, Post-synthetic modified MOF for Sonogashira cross-coupling and Knoevenagel condensation reactions, *J. Catal.* 344 (2016) 445–454.
- [3] J. van Schijndel, L.A. Canalle, D. Molendijk, J.J.J.G.C.L. Meuldijk, Reviews, the Green Knoevenagel Condensation: Solvent-free Condensation of Benzaldehydes, vol. 10, 2017, pp. 404–411.
- [4] S. Qi, S. Lan-Xiang, G. Ze-Mei, C. Tie-Ming, L. Run-Tao, An Efficient and Green Procedure for the Knoevenagel Condensation Catalyzed by Urea, vol. 23, 2005, pp. 745–748.
- [5] J.S. Sandhu Suresh, Recent advances in ionic liquids: green unconventional solvents of this century: part I, *Green Chem. Lett. Rev.* 4 (2011) 289–310.
- [6] T.G. Bonner, P. McNamara, The pyridine-catalysed acetylation of phenols and alcohols by acetic anhydride, *J. Chem. Soc. B Phys. Org.* (1968) 795–797.
- [7] E.F.V. Scriven, 4-Dialkylaminopyridines: super acylation and alkylation catalysts, *Chem. Soc. Rev.* 12 (1983) 129–161.
- [8] A.R. Gholap, K. Venkatesan, T. Daniel, R.J. Lahoti, K.V. Srinivasan, Ultrasound promoted acetylation of alcohols in room temperature ionic liquid under ambient conditions, *Green Chem.* 5 (2003) 693–696.
- [9] A.K. Chakraborti, R. Gulhane, Perchloric acid adsorbed on silica gel as a new, highly efficient, and versatile catalyst for acetylation of phenols, thiols, alcohols, and amines, *Chem. Commun.* (2003) 1896–1897.
- [10] G. Bartoli, R. Dalpozzo, A. De Nino, L. Maiuolo, M. Nardi, A. Procopio, A. Tagarelli, Per-O-acetylation of sugars catalyzed by Ce(OTf)₃, *Green Chem.* 6 (2004) 191–192.
- [11] R. Alletti, M. Perambuduru, S. Samantha, V.P. Reddy, Gadolinium triflate: an efficient and convenient catalyst for acetylation of alcohols and amines, *J. Mol. Catal. Chem.* 226 (2005) 57–59.
- [12] Z. Liu, Q. Ma, Y. Liu, Q. Wang, 4-(N,N-Dimethylamino)pyridine hydrochloride as a recyclable catalyst for acylation of inert alcohols: substrate scope and reaction mechanism, *Org. Lett.* 16 (2014) 236–239.
- [13] B.M. Reddy, P.M. Sreekanth, P. Lakshmanan, Sulfated zirconia as an efficient catalyst for organic synthesis and transformation reactions, *J. Mol. Catal. Chem.* 237 (2005) 93–100.
- [14] C.W. Lim, I.S. Lee, Magnetically recyclable nanocatalyst systems for the organic reactions, *Nano Today* 5 (2010) 412–434.
- [15] S.B. Somwanshi, S.B. Somvanshi, P.B. Kharat, Nanocatalyst: a brief review on synthesis to applications, *J. Phys. Conf.* 1644 (2020) 012046.
- [16] M.B. Gawande, R.K. Pandey, R.V. Jayaram, Role of mixed metal oxides in catalysis science—versatile applications in organic synthesis, *Catal. Sci. Technol.* 2 (2012) 1113–1125.
- [17] L.L. Chng, N. Erathodiyil, J.Y. Ying, Nanostructured catalysts for organic transformations, *Accounts Chem. Res.* 46 (2013) 1825–1837.
- [18] M.B. Gawande, S.N. Shelke, R. Zboril, R.S. Varma, Microwave-Assisted chemistry: synthetic applications for rapid assembly of nanomaterials and organics, *Accounts Chem. Res.* 47 (2014) 1338–1348.
- [19] J. Safaei-Ghomi, H. Shahbazi-Alavi, S. Kalhor, CeO₂ nanoparticles: an efficient and robust catalyst for the synthesis of 2-amino-4,6-diarylbenzene-1,3-dicarbonitriles, *Monatshfte für Chemie - Chemical Monthly* 147 (2016) 1933–1937.
- [20] nbsp Suresh, J.S. Sandhu, ZnO nanobelts: an efficient catalyst for synthesis of 5-arylidine-2,4-thiazolidinediones and 5-arylidine-rhodanines, *J International Journal of Organic Chemistry* 02No.03 (2012) 6.
- [21] S. Shabalala, S. Maddila, W.E. van Zyl, S.B. Jonnalagadda, Sustainable CeO₂/ZrO₂ mixed oxide catalyst for the green synthesis of highly functionalized 1,4-Dihydropyridine-2,3-dicarboxylate derivatives, *Curr. Org. Synth.* 15 (2018) 396–403.
- [22] F. Yin, D. Ye, C. Zhu, L. Qiu, Y. Huang, Stretchable, highly durable ternary nanocomposite strain sensor for structural health monitoring of flexible aircraft, *Sensors* 17 (2017) 2677.
- [23] G. Zamiri, A.S.M.A. Haseeb, P. Jagadish, M. Khalid, I. Kong, S.G. Krishnan, Three-dimensional graphene-TiO₂-SnO₂ ternary nanocomposites for high-performance asymmetric supercapacitors, *ACS Omega* 7 (2022) 43981–43991.
- [24] J.N. Appaturi, R. Ratti, B.L. Phoon, S.M. Batagarawa, I.U. Din, M. Selvaraj, R.J. Ramalingam, A review of the recent progress on heterogeneous catalysts for Knoevenagel condensation, *Dalton Trans.* 50 (2021) 4445–4469.
- [25] H. Jing, X. Wang, Y. Liu, A. Wang, Preparation of magnetic nanocomposites of solid acid catalysts and their applicability in esterification, *Chin. J. Catal.* 36 (2015) 244–251.
- [26] S. Wang, Z. Ren, W. Cao, W. Tong, The Knoevenagel condensation of aromatic aldehydes with malononitrile or ethyl cyanoacetate in the presence of ctmb in water, *Synth. Commun.* 31 (2001) 673–677.
- [27] Y. Zhang, T. Dai, F. Zhang, J. Zhang, G. Chu, C. Quan, Fe₃O₄@UiO-66-NH₂ core-shell nanohybrid as stable heterogeneous catalyst for Knoevenagel condensation, *Chin. J. Catal.* 37 (2016) 2106–2113.
- [28] P. Basu, P. Bhanja, N. Salam, T.K. Dey, A. Bhaumik, D. Das, S.M. Islam, Silver nanoparticles supported over Al₂O₃@Fe₂O₃ core-shell nanoparticles as an efficient catalyst for one-pot synthesis of 1,2,3-triazoles and acylation of benzyl alcohol, *Mol. Catal.* 439 (2017) 31–40.
- [29] S. Liu, H. Chen, H. Lv, Q.P. Qin, L. Fan, X. Zhang, Chemorobust 4p-5p {InPb}-organic framework for efficiently catalyzing cycloaddition of CO₂ with epoxides and deacetalization-Knoevenagel condensation, *Mater. Today Chem.* 24 (2022) 100984.
- [30] X. Zhang, X. Wang, C. Li, T. Hu, L. Fan, Nanoporous {Co₃}-Organic framework for efficiently separating gases and catalyzing cycloaddition of epoxides with CO₂ and Knoevenagel condensation, *J. Colloid Interface Sci.* 656 (2024) 127–136.
- [31] A. Gogoi, K.C. Sarma, Synthesis of the novel β-cyclodextrin supported CeO₂ nanoparticles for the catalytic degradation of methylene blue in aqueous suspension, *Mater. Chem. Phys.* 194 (2017) 327–336.
- [32] Y. Bi, S. Ouyang, J. Cao, J. Ye, Facile synthesis of rhombic dodecahedral AgX/Ag₃PO₄ (X = Cl, Br, I) heterocrystals with enhanced photocatalytic properties and stabilities, *Phys. Chem. Chem. Phys.* 13 (2011) 10071–10075.
- [33] V. Singh, P.K. Sharma, P. Chauhan, Synthesis of CdS nanoparticles with enhanced optical properties, *Mater. Char.* 62 (2011) 43–52.
- [34] Y. Song, H. Zhao, Z. Chen, W. Wang, L. Huang, H. Xu, H. Li, The CeO₂/Ag₃PO₄ Photocatalyst with Stability and High Photocatalytic Activity under Visible Light Irradiation, vol. 213, 2016, pp. 2356–2363.
- [35] S. Ijaz, M.F. Ehsan, M.N. Ashiq, N. Karamat, T. He, Preparation of CdS@CeO₂ core/shell composite for photocatalytic reduction of CO₂ under visible-light irradiation, *Appl. Surf. Sci.* 390 (2016) 550–559.
- [36] U. Sulaeman, S. Suhendar, H. Diastuti, A. Riapanitra, S. Yin, Design of Ag₃PO₄ for highly enhanced photocatalyst using hydroxyapatite as a source of phosphate ion, *Solid State Sci.* 86 (2018) 1–5.

- [37] Z. Chen, S. Liu, M.-Q. Yang, Y.-J. Xu, Synthesis of uniform CdS nanospheres/graphene hybrid nanocomposites and their application as visible light photocatalyst for selective reduction of nitro organics in water, *ACS Appl. Mater. Interfaces* 5 (2013) 4309–4319.
- [38] E. Mohammadiyan, H. Ghafuri, A. Kakanejadifard, Synthesis and characterization of a magnetic Fe₃O₄@CeO₂ nanocomposite decorated with Ag nanoparticle and investigation of synergistic effects of Ag on photocatalytic activity, *Optik* 166 (2018) 39–48.
- [39] G. Postole, B. Chowdhury, B. Karmakar, K. Pinki, J. Banerji, A. Auroux, Knoevenagel condensation reaction over acid–base bifunctional nanocrystalline CexZr1–xO₂ solid solutions, *J. Catal.* 269 (2010) 110–121.
- [40] H. Kargar, F. Ghasemi, M. Darroudi, Bioorganic polymer-based synthesis of cerium oxide nanoparticles and their cell viability assays, *Ceram. Int.* 41 (2015) 1589–1594.
- [41] A.S. Tofik, A.M. Taddesse, K.T. Tesfahun, G.G. Girma, Fe–Al binary oxide nanosorbent: synthesis, characterization and phosphate sorption property, *J. Environ. Chem. Eng.* 4 (2016) 2458–2468.
- [42] P. Bhanja, U. Kayal, A. Bhaumik, Ordered mesoporous γ -Al₂O₃ as highly efficient and recyclable catalyst for the Knoevenagel reaction at room temperature, *Mol. Catal.* 451 (2018) 220–227.
- [43] L. Vivier, D. Duprez, *Ceria-Based Solid Catalysts for Organic Chemistry*, vol. 3, 2010, pp. 654–678.
- [44] L.C. Player, B. Chan, P. Turner, A.F. Masters, T. Maschmeyer, Bromozincate ionic liquids in the Knoevenagel condensation reaction, *Appl. Catal. B Environ.* 223 (2018) 228–233.
- [45] S. Rathod, M. Navgire, B. Arbad, M. Lande, Preparation of Mg-doped Ce-Zr solid catalysts and their catalytic potency for the synthesis of 5-arylidene-2,4-thiazolidinediones via Knoevenagel condensation %J South African, *J. Chem.* 65 (2012) 196–201.
- [46] C. Mukhopadhyay, A. Datta, A. Simple, Efficient and green procedure for the Knoevenagel condensation of aldehydes with N-methylpiperazine at room temperature under solvent-free conditions, *Synth. Commun.* 38 (2008) 2103–2112.
- [47] F. Hajizadeh, B. Maleki, F.M. Zonoz, A. Amiri, Application of structurally enhanced magnetite cored polyamidoamine dendrimer for Knoevenagel condensation, *J. Iran. Chem. Soc.* 18 (2021) 793–804.
- [48] G. Han, J. Du, L. Chen, L. Zhao, Synthesis and Characterization of 11-Amino-3-methoxy-8-substituted-12-aryl-8,9-dihydro-7H-chromeno[2,3-b]quinolin-10(12H)-one Derivatives 51 (2014) 1094–1099.
- [49] M.A. Gouda, A.A. Abu-Hashem, An eco-friendly procedure for the efficient synthesis of arylidinemalononitriles and 4,4'-(arylmethylene)bis(3-methyl-1-phenyl-1H-pyrazol-5-ols) in aqueous media, *Green Chem. Lett. Rev.* 5 (2012) 203–209.
- [50] G. Li, J. Xiao, W. Zhang, Knoevenagel condensation catalyzed by a tertiary-amine functionalized polyacrylonitrile fiber, *Green Chem.* 13 (2011) 1828–1836.
- [51] Q. Xu, Y. Niu, G. Wang, Y. Li, Y. Zhao, V. Singh, J. Niu, J. Wang, Polyoxoniobates as a superior Lewis base efficiently catalyzed Knoevenagel condensation, *Mol. Catal.* 453 (2018) 93–99.
- [52] F. Zamani, E. Izadi, Polyvinyl amine coated Fe₃O₄@SiO₂ magnetic microspheres for Knoevenagel condensation, *Chin. J. Catal.* 35 (2014) 21–27.
- [53] W. Zhang, J. Liang, Y. Liu, S. Sun, X. Ren, M. Jiang, Knoevenagel condensation reaction over acid-base bifunctional MgO/HMCM-22 catalysts, *Chin. J. Catal.* 34 (2013) 559–566.
- [54] S.M. Islam, A.S. Roy, R.C. Dey, S. Paul, Graphene based material as a base catalyst for solvent free Aldol condensation and Knoevenagel reaction at room temperature, *J. Mol. Catal. Chem.* 394 (2014) 66–73.
- [55] S. Farhadi, K. Jahanara, ZnAl₂O₄@SiO₂ nanocomposite catalyst for the acetylation of alcohols, phenols and amines with acetic anhydride under solvent-free conditions, *Chin. J. Catal.* 35 (2014) 368–375.
- [56] A. Amić, M. Molnar, An improved and efficient N-acetylation of amines using choline chloride based deep eutectic solvents, *Org. Prep. Proced. Int.* 49 (2017) 249–257.
- [57] U.P. Saikia, F.L. Hussain, M. Suri, P. Pahari, Selective N-acetylation of aromatic amines using acetonitrile as acylating agent, *Tetrahedron Lett.* 57 (2016) 1158–1160.
- [58] A. Dixit, P. Sharma, Kumar, synthesis & characterization of 4- HYDROXYACETANILIDE starting from acetanilide, *Journal of Medical Pharmaceutical And Allied Sciences* (2016) 73–77.
- [59] M. Brahmayya, S.-Y. Suen, S.A. Dai, Sulfonated graphene oxide-catalyzed N-acetylation of amines with acetonitrile under sonication, *J. Taiwan Inst. Chem. Eng.* 83 (2018) 174–183.
- [60] S.M. Mali, R.D. Bhaire, H.N. Gopi, Thioacids mediated selective and mild N-acylation of amines, *J. Org. Chem.* 78 (2013) 5550–5555.
- [61] S. Farhadi, M. Zaidi, Bismuth ferrite (BiFeO₃) nanopowder prepared by sucrose-assisted combustion method: a novel and reusable heterogeneous catalyst for acetylation of amines, alcohols and phenols under solvent-free conditions, *J. Mol. Catal. Chem.* 299 (2009) 18–25.
- [62] L. Osiglio, G. Romanelli, M. Blanco, Alcohol acetylation with acetic acid using borated zirconia as catalyst, *J. Mol. Catal. Chem.* 316 (2010) 52–58.
- [63] A.B. Majumder, B. Singh, D. Dutta, S. Sadhukhan, M.N. Gupta, Lipase catalyzed synthesis of benzyl acetate in solvent-free medium using vinyl acetate as acyl donor, *Bioorg. Med. Chem. Lett.* 16 (2006) 4041–4044.
- [64] M.N. Rashed, S.M.A.H. Siddiki, A.S. Touchy, M.A.R. Jamil, S.S. Poly, T. Toyao, Z. Maeno, K.-i. Shimizu, Direct Phenolysis Reactions of Unactivated Amides into Phenolic Esters Promoted by a Heterogeneous CeO₂ Catalyst, vol. 25, 2019, pp. 10594–10605.
- [65] E. Mohsen, S.A. Reza, H. Hamed, Fe₃O₄@SiO₂/Schiff base complex of Co(II) as an efficient Lewis acid nanocatalyst for acetylation of alcohols and phenols under solvent-free conditions, *Iran. J. Sci. Technol. Trans. A-Science* 41 (2017) 735–747.
- [66] A.R. Hajipour, H. Karimi, Acetylation of alcohols and phenols under solvent-free conditions using copper zirconium phosphate, *Chin. J. Catal.* 35 (2014) 1982–1989.